DALTON
FULL PAPER

Raman spectroscopic studies of molten ZrF_4–KF mixtures and of A_2ZrF_6, A_3ZrF_7 (A = Li, K or Cs) compounds

V. Dracopoulos, J. Vagelatos and G. N. Papatheodorou *

Department of Chemical Engineering, University of Patras & Institute of Chemical Engineering and High Temperature Chemical Processes (ICE/HT-FORTH), P.O. Box 1414, GR-26500, Rio, Greece. E-mail: gpap@iceht.forth.gr

Received 19th October 2000, Accepted 9th February 2001
First published as an Advance Article on the web 15th March 2001

Raman spectra of ZrF_4–KF molten mixtures have been measured at compositions up to 66 mol% ZrF_4 and at temperatures up to 1000 °C. The data indicate that in mixtures rich in alkali fluoride two kinds of chemical species predominate the melt structure; octahedral ZrF_6^{2-} ($\nu_1(A_{1g})$ 570 cm^{-1} and ν_5 (F_{2g}) 248 cm^{-1}) and pentagonal bipyramidal ZrF_7^{3-} ($\nu_1(A_1')$ 535 cm^{-1} and $\nu_9(E_2')$ 340 cm^{-1}). An equilibrium between the two species is established which depends on temperature and composition. Spectral changes upon melting A_2ZrF_6 (A = Li or K) and A_3ZrF_7 (A = K or Cs) polycrystalline compounds support the proposed two species equilibrium scheme. At 33 mol% ZrF_4 the predominant species present are ZrF_6^{2-} octahedra. With increasing ZrF_4 mole fraction the strong $\nu_1(A_{1g})$ band at 570 cm^{-1} shifts continuously to higher wavenumbers and new bands appear in the spectra. At the maximum composition studied of 66 mol% ZrF_4 the spectra are characterized by two polarized (630 cm^{-1}, strong and ≈500 cm^{-1}, weak) and two weak depolarized bands (245 and ≈180 cm^{-1}). The observed spectral trends with variation of composition are similar to those found for $ThCl_4$–CsCl molten mixtures and are interpreted with an analogous model where the structure of the rich in ZrF_4 melts is dominated by small size chains formed by "ZrF_6" octahedra bound by corners and/or edges.

Introduction

In two recent publications we have used Raman spectroscopy to investigate the structural properties of two sets of molten binary mixtures $ZrCl_4$–ACl[1] and $ThCl_4$–ACl[2] (A = Li, Na, K or Cs). For both binaries it was found that in mixtures rich in alkali metal chloride the predominant species present are the MCl_6^{2-} (M = Zr or Th) octahedra. However, in the case of $ThCl_4$ an equilibrium of the type $ThCl_7^{3-} \rightleftharpoons ThCl_6^{2-} + Cl^-$ is established in the very rich in alkali metal chloride mixtures. As the mixtures became more concentrated in tetravalent chloride the structural behaviors of the two sets of binaries deviate drastically from each other. Thus, as the $ZrCl_4$ mole fraction increases other zirconium chloroanions (*i.e.* $Zr_2Cl_6^{2-}$, $Zr_2Cl_{10}^{2-}$/$ZrCl_5^-$) are formed. At high $ZrCl_4$ mole fractions an equilibrium exists between $Zr_2Cl_9^-$ and monomeric and/or polymeric $(ZrCl_4)_n$ species.[1] The structure of pure molten $ZrCl_4$ is also described with an equilibrium molecular mixture of $ZrCl_4$ monomers and $(ZrCl_4)_n$ oligomers ($n = 2$ or 6). On the other hand, it appears that the structure of the binaries involving $ThCl_4$ yield at high $ThCl_4$ content octahedral chain species of the type $[Th_nCl_{4n+2}]^{2-}$ and $[Th_nCl_{4n-2}]^{2+}$ where the end Th atoms are six- and four-fold coordinated for the chain anion and cation respectively. It has been also argued that pure molten $ThCl_4$ is self ionized to form the above chain species.[2]

The purpose of the present work is to extend the above studies to fluoride melts. The binary system ZrF_4–AF (A mainly K) was chosen for several reasons. First it is an extension of the corresponding chloride system and has a ratio of ionic radii Zr^{4+} : F^- almost equal to that of Th^{4+} : Cl^-; thus it will be interesting to examine any structural similarities between these systems. In addition the co-ordination geometries of Zr^{4+} in molten ZrF_4–NaF–LiF mixtures have been investigated by Raman spectroscopy in an early work of Toth *et al.*[3] It was proposed that in these mixtures and at ZrF_4 mole fractions up to 33% the main species present are ZrF_8^{4-}, ZrF_7^{3-} and ZrF_6^{2-}.

Finally, zirconium(IV) fluoride is one of the main components in fluorozirconate glasses which are rather important materials for the development of optical components including optical fibers.[4] These glasses contain ZrF_4 in a composition range ≈50–70 mol% plus two or more fluorides like BaF_2, LaF_3, ThF_4, PbF_2, NaF. The structural properties of these multicomponent glasses and their corresponding melts have been the subject of numerous investigations. Based on Raman spectroscopic studies Almeida and co-workers[5–7] have suggested that in the glass the zirconium(IV) forms chains of ZrF_6^{2-} octahedra sharing corners. Further, vibrational spectroscopy studies,[8–10] X-ray diffraction[11–13] and molecular simulations[14,15] have proposed that in the glass zirconium(IV) polyhedra with seven or eight fluorides are formed which may share edges or corners. Similar views have been supported by EXAFS studies.[16–18] In a detailed Raman spectroscopic study of fluorozirconate glasses and melts involving BaF_2 and PbF_2 Walrafen *et al.*[19] suggested the formation of network structures involving ZrF_n ($n = 5$, 6, 7 or 8) polyhedra sharing corners and/or edges. Upon melting the glass the network presumably breaks up giving anions of the type ZrF_5^-, ZrF_6^{2-} and ZrF_7^{3-}. Also, it has been suggested that on going from the glass to the melt the degradation of the network is followed by a decrease in the zirconium(IV) coordination.[20]

Certain conclusions from the above studies have been supported by independent thermodynamic investigations.[21,22] However, most of these glasses and melts studied, apart from ZrF_4, contained a variety of other metal fluorides and thus the establishment of structural systematics that depend only on the composition of a simple binary was not possible.

The work reported here concerns the Raman spectra of the ZrF_4–KF molten mixtures and aims to establish the spectral and structure changes occurring in this binary with composition and temperature. Furthermore, the spectral changes occurring upon melting the A_2ZrF_6 (A = Li or K) and A_3ZrF_7 (A = K or Cs) polycrystalline compounds have been measured and compared with literature data.[23] The data are used in order to identify the predominant structural units present in these melts and the structural variations occurring upon melting.

Experimental

Zirconium(IV) fluoride was purchased from Alfa Inorganic Co. (99.9%) and was further purified by sublimation into a graphite tube with a top cover in an inert atmosphere high temperature furnace. The oxide content of the final product was measured by LECO apparatus to be around 100 ppm. The LiF, KF and CsF (99%) were purchased from Merck Co. and purified by slow crystallization from the melt in an inert atmosphere furnace. For the crystallization process a vitreous carbon crucible was used for LiF and KF and a platinum crucible for CsF.

All room temperature operations were carried out in an argon filled glove box with O_2 and/or H_2O content less than 1 ppm. Mixtures with appropriate concentrations were prepared and melted under an argon atmosphere in an electrical furnace in order to ensure homogeneity. The congruent melting compounds Li_2ZrF_6, K_3ZrF_7 and Cs_3ZrF_7 were prepared by mixing appropriate stoichiometric quantities, melting for several minutes under an argon atmosphere and then cooling to room temperature. The incongruently melting K_2ZrF_6 solid compound was prepared by dissolving stoichiometric amounts of KF and ZrF_4 in 40% HF solution (in excess). The white needle crystals so obtained gave Raman spectra (see next section) identical to those reported for K_2ZrF_6 crystals.[3]

The spectra were excited with a Spectra Physics Model 2017 argon ion laser. Scattered light was collected at right angles to the incident beam and analysed by a Jobin-Yvon T6400 monochromator in the triple configuration. The monochromator was equipped with a liquid nitrogen cooled CCD detector. The spectral window was centered at 450 cm^{-1} relative to the excitation line and the opening window was ≈770 cm^{-1}. The integration time was 5 s while the slit opening was at 300 μm. For the melts, two polarization configurations were used by means of polarization of the incident-scattered light, namely VV (vertical–vertical) and HV (horizontal–vertical). For the polycrystalline solids no polarization measurements were possible. Before each high temperature experiment the optical scattering geometry was aligned with a CCl_4 sample at room temperature and with a $ZnCl_2$–CsCl mixture at ≈700 °C. The furnace used for the measurements was a home made optical furnace[24] equipped with an OMEGA CN4801 microcontroller. The temperature was measured with a Pt-Pt10Rh thermocouple at the bottom of the cell and the temperature gradient at the optical openings of the furnace was ≈5 °C.

The windowless graphite cell technique used for recording spectra of fluoride melts has been described elsewhere.[25] The amounts of salts placed in the cell were adjusted so that after melting the liquid droplet formed was in the center of cell at the level of the optical paths. After filling the cell and before melting the sample, the cell was placed and sealed in a fused silica tube under ≈0.8 atm of high purity Ar.

Results and discussion

Raman spectra of the ZrF_4–KF binary were recorded at different compositions and temperatures as listed in Table 1. It was observed that at ZrF_4 compositions above 66 mol% the vapor pressure of ZrF_4 over the molten mixture (with liquidus temperatures above 700 °C) is rather high (a few Torr). The vapors so formed reacted with the fused silica tube surrounding the graphite cell creating a milky surface which blocked the optical paths of the experiment. Thus, it was not possible to record spectra at $x_{ZrF_4} > 0.66$. Spectra were also measured for the polycrystalline compounds Li_2ZrF_6, K_2ZrF_6, K_3ZrF_7 and Cs_3ZrF_7 from liquid nitrogen temperature up to and over the congruent melting points. In most cases the spectra of all molten and solid samples studied here were measured more than once in separate experiments.

Changes of vibrational modes upon melting binary compounds

The phase diagrams of the ZrF_4–AF (A = alkali metal) systems show the formation of over 25 binary compounds with congruent or incongruent melting points.[26] Depending on the stoichiometry and the alkali metal a variety of structures are formed having the zirconium(IV) in different site symmetries or in "isolated" polyhedra with defined coordination numbers which in all cases studied so far vary from six to eight. The binary compounds chosen to investigate, Li_2ZrF_6, K_2ZrF_6 and K_3ZrF_7, have known crystal structures where the zirconium(IV) is surrounded by six,[27] eight[28] and seven[29] fluoride ions respectively. The crystal structure of the fourth compound studied, Cs_3ZrF_7, is not well known but it was found from its Raman spectrum to have a structure rather close to that of K_3ZrF_7.

It was anticipated that from the solid spectra the frequency of the Zr–F stretching vibration in different fluoride geometries could be defined and compared with the corresponding frequency in the melt. In many respects such a comparison may be correct when isolated ZrF_n (n = 6, 7 or 8) units exist in the solid. On the other hand if strong sharing (bridging) of the fluoride occurs between neighboring zirconium(IV) atoms a proper comparison cannot be made but observations of frequency shifts upon melting may help in defining an increase/decrease in the coordination of zirconium(IV).

Li_2ZrF_6. The crystal structure of Li_2ZrF_6 possesses hexagonal $P\bar{3}1m(D_{3d}^{1})$ symmetry.[27] The crystal is built up by isolated distorted (D_{3d}) ZrF_6^{2-} octahedra. Each corner of ZrF_6^{2-} is shared by two Li^+ octahedra that share edges with each other. The

Table 1 Main Raman bands observed for ZrF_4–AF molten mixtures at different compositions and temperatures

System (mol% ZrF_4)	T/°C	Main bands (cm^{-1})[a,b] P[c]	DP[d]
$LiF–ZrF_4$			
33	750	585	240
$KF–ZrF_4$			
7	900	570	248
		535	(340)
	1000	570	248
		(535)	(340)
14	850	(650)	
		570	248
		535	(340)
	900	(650)	
		570	248
		535	(340)
	950	(650)	
		570	248
		(535)	(340)
	1000	(650)	
		570	248
		(535)	(340)
25	1000	(650)	
		570	248
		(535)	
33	850	570	248
	900	570	248
42	750	592	248
			(180)
50	750	604	245
			180
66	820	630	(245)
		(500)	180
			(600)
$CsF–ZrF_4$			
25	850	563	240
		(520)	

[a] Estimated error ± 1 cm^{-1}. [b] Numbers in parentheses indicate broad or shoulder bands with an estimated error of ±10 cm^{-1}. [c] P = Polarized. [d] DP = Depolarized.

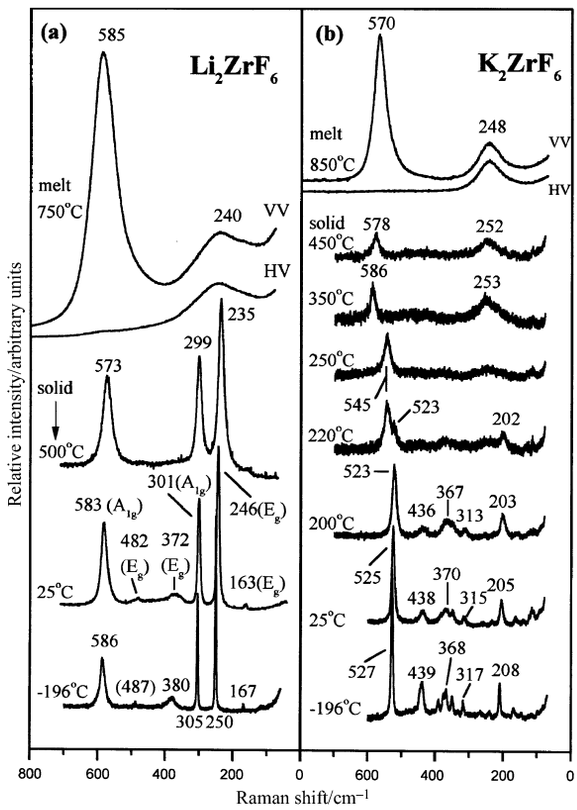

Fig. 1 Raman spectra of A_2ZrF_6 (A = Li or K) polycrystalline solids from liquid nitrogen temperature to temperatures above melting. Conditions: (a) solids, $\lambda_0 = 514.5$ nm, laser power (LP) = 200 mW, integration time (IT) = 20 s, spectral slit width (ssw) = 2 cm^{-1}; (b) melt, $\lambda_0 = 488$ nm, LP = 500 mW, IT = 5 s, ssw = 5–6 cm^{-1}.

compound melts congruently[26] without any phase transitions from liquid nitrogen temperatures to the melting point.

A factor group analysis gives the representation: $\Gamma_{3N} = 2A_{1g}(R) + 4E_g(R) + 2A_{2g}(IR) + A_{1u}(IA) + 5A_{2u}(IR) + 6E_u(IR)$. Four from the predicted six Raman active modes are the internal modes for the ZrF_6^{2-} distorted octahedron ($\Gamma_{D_{3d}}(R) = 2A_{1g} + 2E_g$). The other two are a translatory mode for the $Li^+(E_g)$ and a librational mode (E_g) for the octahedron. All six modes are observed in the solid spectra and their assignments are shown in Fig. 1(a). The spectra and assignments given here are quite similar to those reported by Toth and Bates.[23] However, we did not observe two bands at 505 and 610 cm^{-1} reported in the latter work. The two low frequency internal modes of the distorted ZrF_6^{2-} octahedra, A_{1g} (305 cm^{-1}) and E_g (250 cm^{-1}), arise from splitting of the ν_5 (F_{2g}) mode of the undistorted octahedra ($\Gamma_{O_h}(R) = A_{1g} + E_g + F_{2g}$). Assuming an

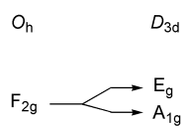

equal weight splitting we can calculate that for the undistorted octahedra $\nu_5(F_{2g}) \approx 277$ cm^{-1} which in combination with the $\nu_1(A_{1g}) = 586$ cm^{-1} mode permits estimation of the $\nu_2(E_g)$ mode of the octahedra from the relation:[30] $\nu_2 \approx \sqrt{\nu_1^2 - 1.5\nu_5^2} = 480$ cm^{-1}. This value is very close to that of the E_g (487 cm^{-1}) mode seen in the spectra (Fig. 1a) for the distorted ZrF_6^{2-} octahedra and further justifies the assignments given here.

With increasing temperature all vibrational modes of the crystal shift to lower frequencies by a few wavenumbers (Fig. 1a). Upon melting the $\nu_1(A_{1g})$ mode exhibits an ≈5 cm^{-1} blue shift while the intense lower frequency bands (E_g and A_{1g}) are substituted in the melt by a broad depolarized band at ≈240 cm^{-1}. It seems that the intense modes of the solid are transferred into the melt. The situation resembles that observed on melting a large number of crystalline compounds containing isolated octahedra (see refs. 1, 2, 31). We thus suggest that the predominant species present in molten Li_2ZrF_6 are ZrF_6^{2-} octahedra giving rise to two vibrational modes $\nu_1(A_{1g})$ 585 cm^{-1} and $\nu_5(F_{2g})$ 240 cm^{-1}. The third expected Raman active mode has a rather weak intensity[31] but its position can be predicted as above[30] at $\nu_2(E_g) \approx 500$ cm^{-1}. Finally, it is noteworthy that the Zr–F stretching mode (A_{1g}) inverses its intensity relative to the F_{2g} ($A_g + E_g$) mode on going from the solid to the melt. This behavior has been also observed in the case of Cs_2ZrCl_6 spectra and an account is given elsewhere.[1]

K_2ZrF_6. The crystal structure of K_2ZrF_6 at room temperature has monoclinic C_{2h}^6 ($C2/c$) symmetry with the zirconium(IV) surrounded by eight fluorine atoms in a C_{2h} site.[28] The vibrational modes span the representation: $\Gamma_{3N} = 13A_g(R) + 14B_g(R) + 13A_u(IR) + 14B_u(IR)$. From the expected 27 Raman active modes only 12 are seen in the spectra of the polycrystalline solid (Fig. 1b). In the absence of single crystal data no assignments can be made. However, the high frequency intense band at 525 cm^{-1} is presumably associated with a Zr–F stretching frequency of the eightfold coordinated unit. These units are not isolated but share bridging fluorides with neighboring zirconium(IV) atoms.[28] The ZrF_4–KF phase diagram shows that K_2ZrF_6 exhibits a phase transformation at ≈130 °C while an incongruent melting point and a partial transformation to K_3ZrF_7 occur at ≈590 °C.[26] At 40 mol% ZrF_4 the $K_3Zr_2F_{11}$ compound is also formed, which at either 320 or 420 °C decomposes yielding in part K_2ZrF_6.[26] The temperature dependent spectra (Fig. 1b) indicate changes that are not compatible with the transformations expected from the phase diagram. Thus, the spectral features of the monoclinic form do not change from liquid nitrogen to ≈200 °C. Then between 220 and 250 °C the 523 cm^{-1} band slowly disappears and a new band at ≈545 cm^{-1} predominates. As we argue in the following section, this new band and the two lower intensity bands at ≈330 and 250 cm^{-1} are due to the ZrF_7^{3-} bipyramidal ion formed in the K_3ZrF_7 crystal. This would imply that between 220 and 250 °C decomposition may occur yielding compounds containing the seven-coordinated species. Further increase of temperature to 350 °C changes the spectra yielding a band at ≈585 cm^{-1} and a relatively intense band at ≈250 cm^{-1}; *i.e.* bands that can be associated with the ZrF_6^{2-} octahedra as was found for solid and molten Li_2ZrF_6. A possible scheme giving account of the overall spectral changes would be through solid phase transformations:

$$3K_2ZrF_6 \text{ (monoclinic)} \overset{220\text{–}250\ ^\circ\text{C}}{\rightleftharpoons} K_3ZrF_7 + K_3Zr_2F_{11} \overset{300\text{–}350\ ^\circ\text{C}}{\rightleftharpoons} 3K_2ZrF_6 \text{ (hexagonal)}$$

Thus at ≈220 °C the monoclinic K_2ZrF_6 crystal with an eightfold coordinated zirconium(IV) is decomposed forming two solids where presumably seven-coordinated zirconium(IV) species are present. At higher temperatures the two solids recombine to form a new structure K_2ZrF_6 containing a sixfold coordinated zirconium(IV). The spectrum of the latter structure does not change as the temperature is increased to 450 °C with the exception of a small, but expected, red shift of the ZrF_6^{2-} modes. Upon melting a further red shift occurs for both bands yielding spectra that resemble those of molten Li_2ZrF_6 and showing the two intense modes of the ZrF_6^{2-} octahedra. It seems that the eightfold coordinated zirconium(IV) in the low temperature solid is gradually changing environment with increasing temperature, yielding seven- and six-fold coordinated structures in the solid and finally preserving the sixfold coordinated ZrF_6^{2-} in the melt. On going from the Li_2ZrF_6

Table 2 Main Raman bands (cm^{-1}) and assignments for the seven-coordinated tetravalent compounds at room temperature

Compound	$\nu_1(A_1')$	$\nu_9(E_2')$	$\nu_{10}(E_2')$	$\nu_8(E_1'')$
K_3ZrF_7[a]	544 (10)[b]	385 (1.4)	327 (0.5)	247 (5.5)
Cs_3ZrF_7[c]	533 (10)	374 (1.2)	312 (0.45)	234 (4.5)

[a] Cubic form (*Fm*3*m*).[29] [b] Numbers in parentheses denote for each polycrystalline solid the relative Raman band intensities at 25 °C. [c] Anticipated cubic form.[26]

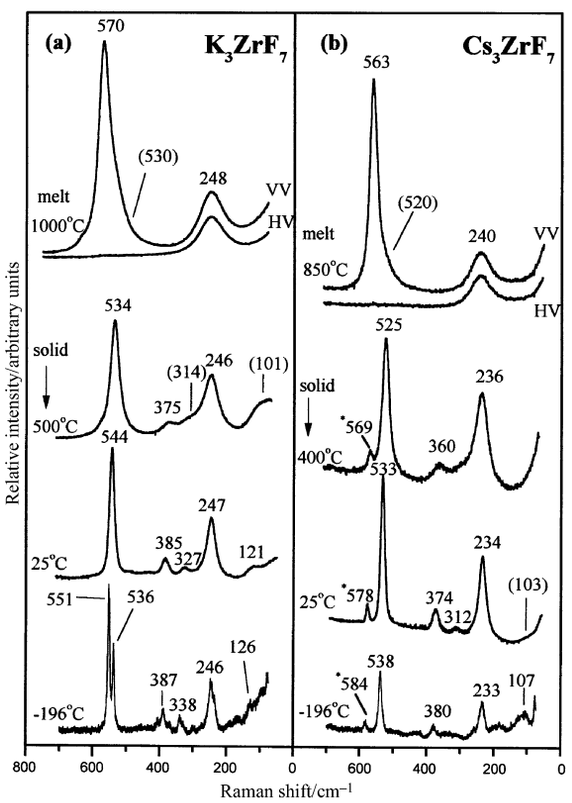

Fig. 2 Raman spectra of A_3ZrF_7 (A = K or Cs) polycrystalline solids from liquid nitrogen temperature to temperatures above melting. Bands noted with an asterisk are presumably due to small amounts of Cs_2ZrF_6.[40] Conditions as in Fig. 1.

to the K_2ZrF_6 melt spectra the $\nu_1(A_{1g})$ octahedral frequency changes by ≈3% (from 585 to 570 cm^{-1}), which is a shift in the same direction and magnitude as observed for the corresponding A_2ThCl_6 (A = Li or K) melts.[2]

K_3ZrF_7, Cs_3ZrF_7. At room temperature the K_3ZrF_7 crystal is cubic (*Fm*3*m*-O_h^5) while at lower temperatures (≈40 °C) a cubic to orthorhombic transformation occurs.[29,32] In both structures ZrF_7^{3-} pentagonal bipyramid (D_{5h}) species exist as isolated complex anions surrounded by the alkali metal cations. A vibrational analysis of these species gives the representation: $\Gamma_{D_{5h}} = 2\ A_1'(R) + E_1''(R) + 2\ E_2'(R) + 2\ A_2''(IR) + 3E_1'(IR) + E_2''$ (IR). As in other cases of crystals containing the MX_7^{3-} ion the Raman spectra show a limited number of bands, most of them due to the internal modes of the pentagonal bipyramid.[2,3,33] The room temperature spectrum of K_3ZrF_7 (Fig. 2a) shows four main bands at 247, 327, 385 and 544 cm^{-1} which in accordance with previous work[2,33] are assigned to the $E_1''(\nu_8)$, 2 $E_2'(\nu_9, \nu_{10})$ and $A_1'(\nu_1)$ modes of the ZrF_7^{3-} complex (see Table 2). At liquid nitrogen temperatures the 545 cm^{-1} band splits into two at 551 and 536 cm^{-1}. Such splitting has previously been seen in the solid state[33] as well as in the vapor and solid spectra of IF_7[34] and is attributed to the separation of

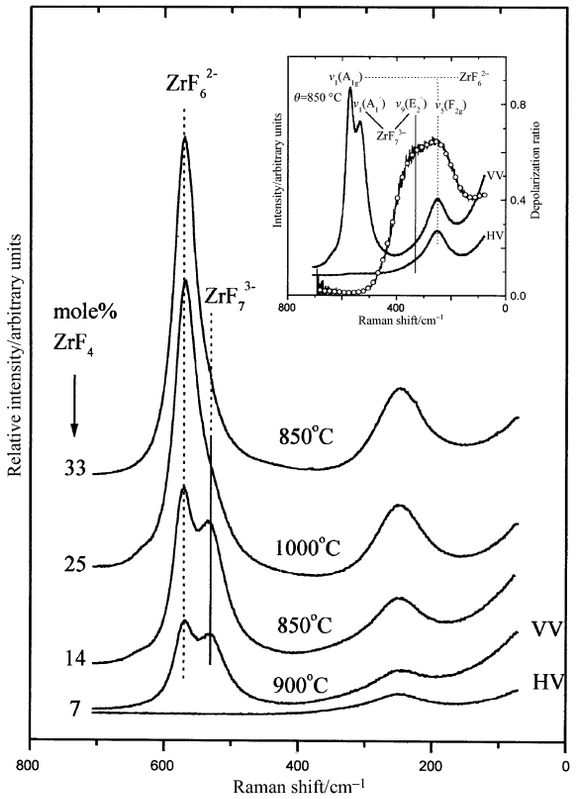

Fig. 3 Composition dependent Raman spectra of $xZrF_4$–$(1 - x)$KF ($0 < x \leq 0.33$) molten mixtures. Inset: Raman VV and HV spectra of $0.14ZrF_4$–0.86KF eutectic mixture at 850 °C. ○, Depolarization ratio. Conditions as in Fig. 1(b).

the axial (ν_1 551 cm^{-1}) and equatorial (ν_2 536 cm^{-1}) symmetric stretching frequencies of the pentagonal bipyramid species.

The room temperature spectrum of Cs_3ZrF_7 also shows four main bands (Fig. 2b, Table 2) having positions and relative intensities similar to those of K_3ZrF_7; this supports the view[26] that the solids are isostructural, containing the ZrF_7^{3-} complex ion whose spectrum predominates for both compounds. The effect of temperature on the Raman spectra of ZrF_7^{3-} (Fig. 2a, 2b) shows the expected trends; *i.e.* band broadening and red frequency shifts with increasing temperature. Thus, the seven-coordinated species is preserved at all temperatures in the solid.

Upon melting both the K_3ZrF_7 and Cs_3ZrF_7 compounds give the same pattern spectra. The $\nu_1(ZrF_7^{3-})$ frequency of the solid shifts to higher energies by ≈30 cm^{-1} in the melt where a new depolarized band at ≈248 cm^{-1} is also present. As in the case of molten Li_2ZrF_6 and K_2ZrF_6 we assign these two bands to the $\nu_1(A_{1g})$ and $\nu_5(F_{2g})$ modes of ZrF_6^{2-}. Thus, it appears that the predominant species in the melts of all four compounds investigated here are the "octahedral" ZrF_6^{2-} species. However, it should be noted that for all four melts (Figs. 1 and 2) the $\nu_1(A_{1g})$ band is rather asymmetric showing a shoulder (band) in the low frequency tail. As we will argue in the following section this band is due ZrF_7^{3-} anion which participates as a minor component in these melts.

The complex anions ZrF_6^{2-} and ZrF_7^{3-} in melt mixtures rich in KF

The spectra of molten mixtures ZrF_4–KF having 25 and 33 mol% ZrF_4 are characterized by two main bands (Fig. 3). Based on the discussion in the previous section we assign these bands to the $\nu_1(A_{1g}) \approx 570$ cm^{-1} and $\nu_5(F_{2g}) \approx 248$ cm^{-1} modes of the ZrF_6^{2-} "octahedra" species. At composition $x_{ZrF_4} < 0.33$ their position does not change but with increasing KF mole fraction the relatively symmetric gaussian shape ν_1 band changes and a

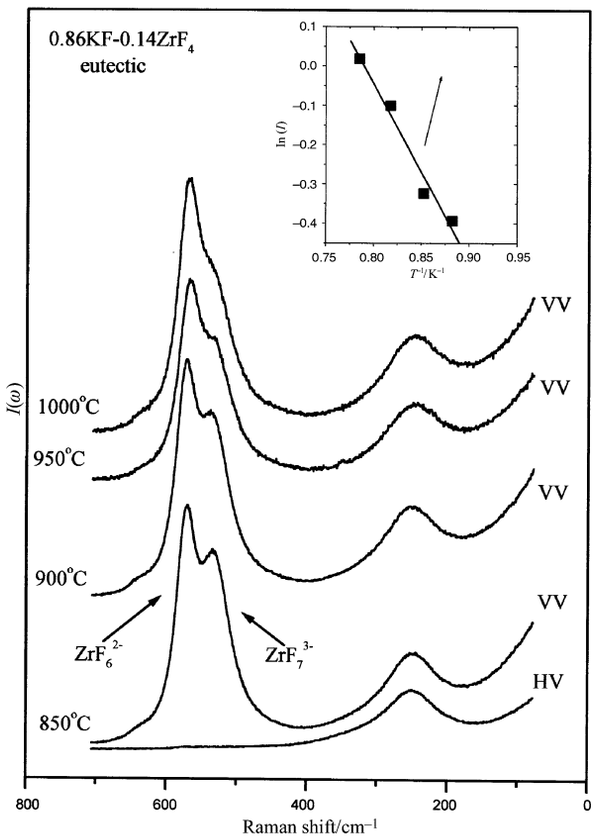

Fig. 4 Temperature dependent spectra of a $0.14ZrF_4$–0.86KF molten eutectic mixture; $I(\omega)$ is the relative Raman intensity. Inset: ΔH calculation from an Arrhenius like plot of $\ln(I)$ *vs.* $1/T$. Conditions as in Fig. 1(b).

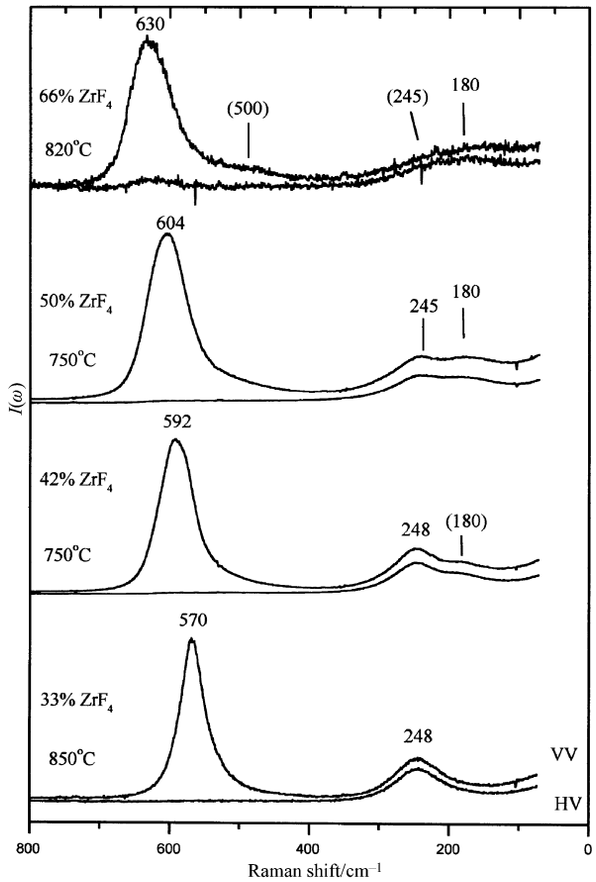

Fig. 5 Composition dependent spectra of $xZrF_4$–$(1 - x)$KF ($0.33 \leq x \leq 0.66$) molten mixtures; $I(\omega)$ is the relative Raman intensity. Conditions as in Fig. 1(b).

shoulder band gradually appears which, at dilute ZrF_4 compositions, gives rise to a well defined polarized band at 535 cm^{-1} (Fig. 3). Two weak shoulder bands at ≈650 and 340 cm^{-1} also appear. The frequency of the new polarized band is at lower energies than that of the $\nu_1(A_{1g})$ ZrF_6^{2-} octahedra and presumably is due to the formation of a new species with coordination higher than six. The data in Table 2 suggest that this new band can be assigned to the $\nu_1(A_1')$ mode of the ZrF_7^{3-} species.

The changes of $\nu_1(A_1')$ and $\nu_1(A_{1g})$ band intensities with composition (Fig. 3) imply that an equilibrium of the type (1)

$$ZrF_7^{3-} \rightleftharpoons ZrF_6^{2-} + F^- \quad (1)$$

is established and that these ionic complexes predominate the melt structure in dilute ZrF_4 compositions. The mixture with $x_{ZrF_4} \approx 0.14$ forms a eutectic and thus it was possible to measure the Raman spectra at different temperatures (Fig. 4). The relative change of the $\nu_1(A_1')$ and $\nu_1(A_{1g})$ band intensities with temperature support the proposed equilibrium (1) and shows that the seven-coordinated species is favored at lower temperatures. From an Arrhenius like plot of the $\nu_1(A_1')/\nu_1(A_{1g})$ relative intensity *vs.* $1/T$ (inset Fig. 4) we can calculate the enthalpy of equilibrium (1) as $\Delta H \approx 37$ kJ mol^{-1}. A value ≈35 kJ mol^{-1} was measured for the corresponding equilibrium in the $ThCl_4$–CsCl system.[2] It is noteworthy that the spectral behavior, the inferred melt structure and the indirect thermodynamic information for $ThCl_4$–CsCl[2] melts are almost identical to those of the ZrF_4–KF system. This is probably due to the similarities of cation/anion ionic radii not only for the tetravalent ($r_{Zr}/r_F \approx r_{Th}/r_{Cl}$) but also for the monovalent ($r_K/r_F \approx r_{Cs}/r_{Cl}$) cations.

The depolarized shoulder band at ≈340 cm^{-1} is mainly seen in the very dilute ZrF_4 spectra and is presumably associated with the ZrF_7^{3-} species. Its presence can be verified from the linear depolarization spectrum (I_{HV}/I_{VV}) which shows (inset Fig. 3) a band in this frequency range. This band is assigned to the $\nu_9(E_2')$ mode of ZrF_7^{3-} in the melt. Finally, the weak shoulder polarized band at ≈650 cm^{-1} is present only in KF containing melts with composition 25 and 14 mol% ZrF_4, and is absent from corresponding melt mixtures of the binary compounds with LiF or CsF. The origin of this band is rather puzzling and we offer no assignment to it.

Associated "octahedral" zirconium fluoride ions in mixtures rich in ZrF_4

The gradual increase of the ZrF_4 mole fraction at compositions above 33 mol% causes several changes in the melt spectra (see Fig. 5) that can be summarized as follows: (i) the $\nu_1(A_{1g})$ 570 cm^{-1} mode of the independent octahedral species becames broader and shifts continuously to higher wavenumbers reaching a value of ≈630 cm^{-1} for the 66 mol% ZrF_4 mixture; (ii) the $\nu_5(F_{2g}) \approx 248$ cm^{-1} mode loses intensity with increasing ZrF_4 content and is slowly substituted by a broader depolarized band with a not well defined maximum at ≈180 cm^{-1} and (iii) a new polarized band appears between 450 and 550 cm^{-1} on the lower energy tail of the main polarized band and a weak depolarized band at ≈600 cm^{-1} occurs in the 66 mol% ZrF_4 mixture.

The above observation suggest that the structure in these melts varies rather continuously and in a manner analogous to that occurring for $ThCl_4$–ACl[2] systems. In contrast there is no similarity with the spectral behavior of the $ZrCl_4$–CsCl system where different zirconium(IV) chloride complex ions in equilibrium were argued to exist.[1]

A possible way to account for the continuous spectral changes is to adapt the model proposed for the $ThCl_4$–ACl systems,[2] where the melt structure is determined by an extended linkage of $ThCl_6^{2-}$ octahedra. In this respect the addition of

ZrF_4 in the 33 mol% mixture, having as predominant species ZrF_6^{2-}, leads to the formation of bioctahedral units where the octahedra are bound by corners or edges. Species like $Zr_2F_{10}^{2-}$ are most probably formed where the Zr–F_t terminal frequency is blue shifted relative to the $\nu_1(A_{1g})$ octahedral frequency due to double bridging within the ion. Thus, the main polarized band in the 42 mol% spectrum (Fig. 5) consist of a superposition of bands due to the Zr–F_t frequency of the "free" octahedra (≈570 cm^{-1}) and the bridge bioctahedra (≈600 cm^{-1}). Furthermore two depolarized bands due to these two species appear in the spectrum at lower frequencies. At 50 mol% the 245 cm^{-1} (ν_5) mode of the "free" octahedra has rather weak intensity and presumably the concentration of these species is very low; in other words the overall spectrum is mainly due to $Zr_2F_{10}^{2-}$ species and the 604 cm^{-1} band is assigned to the Zr–F_t frequency of this ion.

As in the case of the $ThCl_4$–CsCl system further addition of ZrF_4 to the 50 mol% mixture may extend the linkage to form three edge-sharing octahedral species ($Zr_3F_{14}^{2-}$) which reach their maximum concentration at 66 mol% composition. There are four bridging and ten terminal fluorides in such an ion $Zr(F_t)_4[Zr(F_t)_2(F_b)_4]Zr(F_t)_4$, thus the observed band at 630 cm^{-1} presumably covers the Zr–F_t frequency region while the weak polarized shoulder between 450 and 550 cm^{-1} is associated with the Zr–F_b bridging vibrations.

Owing to the vapor pressure of ZrF_4 no measurements were possible for melts with higher than ≈66 mol% ZrF_4. However, the above mentioned similarities of the ZrF_4–KF and $ThCl_4$–CsCl melts from dilute ZrF_4 solution and up to 66 mol% ZrF_4 indicate that the structures of the rich in ZrF_4 melts and of pure molten ZrF_4 may have an octahedral bridged chain character and not a molecular one as in the case of $ZrCl_4$–CsCl melts.[1] Such a chain structure is compatible with model thermodynamic calculations[22] which suggest that, with increasing composition above 33 mol% ZrF_4, doubly charged bridged octahedral ions are formed which increase their chain length in the sequence ZrF_{10}^{2-}, $Zr_3F_{12}^{2-}Cl_6^{2-}$, $Zr_4F_{18}^{2-}$, $Zr_5F_{22}^{2-}$, *etc*. This model could be extended to pure molten ZrF_4 where, in analogy with $ThCl_4$, octahedral charged chains with a higher number of zirconium(IV) atoms may be present. Supporting this view are viscosity measurements of ZrF_4-based melt mixtures which indicate that these melts have a more ionic like behavior and are different than the network like glass formers.[35]

In the solid state ZrF_4 and $ThCl_4$ are polymorphic materials[36,37] forming compact structures where the tetravalent cation is surrounded by eight halide ions shared between neighboring cations. The orientation and packing of the ZrF_8 or $ThCl_8$ triangular dodecahedra determine the details of the polymorphic crystal structures. The entropies of fusion are ≈40 and ≈42 J K^{-1} mol^{-1} for ZrF_4[38] and $ThCl_4$[39] respectively. These values are rather high and within experimental errors very close to each other indicating that the melting of the compact crystals yields similar liquid structures.

All these observations lead to the tentative conclusion that, as in the case of $ThCl_4$,[2] the melting of pure ZrF_4 is probably accompanied by a self dissociation scheme of the type: $nZrF_4 \rightleftharpoons \frac{1}{2}[Zr_nF_{4n-2}]^{2+} + \frac{1}{2}[Zr_nF_{4n+2}]^{2-}$ where the doubly charged ions consist of edge bridged octahedra with the exception of the two end zirconium(IV) atoms of the cation which have a fourfold coordination. If the dissociation is well shifted to the left and the values of n are high then the predominant coordination in molten ZrF_4 is sixfold. Obviously, other more concrete experimental evidence is needed before reaching any definite conclusions. In this respect measurements of electrical conductivity and neutron diffraction studies of molten ZrF_4 would be elucidating.

Acknowledgements

The ZrF_4 samples were prepared and analysed at the Institute of Inorganic Chemistry, Norwegian University of Science and Technology, Trondheim, Norway. Many thanks to Professor T. Østvold and Dr A. F. Vik for guiding and helping one of us (J. V.) in preparing these samples.

References

1 G. M. Photiadis and G. N. Papatheodorou, *J. Chem. Soc.*, *Dalton Trans.*, 1998, 981.
2 G. M. Photiadis and G. N. Papatheodorou, *J. Chem. Soc.*, *Dalton Trans.*, 1999, 3541.
3 L. M. Toth, A. S. Quist and G. E. Boyd, *J. Phys. Chem.*, 1973, **77**, 1384.
4 *Fluoride Glass and Fiber Optics*, eds. I. D. Aggarwal and G. Lu, Academic Press Inc., Boston, 1991.
5 R. M. Almeida and J. D. Mackenzie, *J. Chem. Phys.*, 1981, **74**, 5954.
6 R. M. Almeida and J. D. Mackenzie, *J. Chem. Phys.*, 1983, **78**, 6502.
7 R. M. Almeida, in *Halide Glasses for Fiber Optics*, ed. R. M. Almeida, Martinus Nijhoff, Dordrecht, 1987, p. 57.
8 Y. Kawamoto, *Phys. Chem. Glasses*, 1984, **25**, 88.
9 Y. Kawamoto and F. Sakaguchi, *Bull. Chem. Soc. Jpn.*, 1983, **56**, 2138.
10 S.-H. Ko and R. H. Doremus, *Phys. Chem. Glasses*, 1991, **32**, 196.
11 R. Coupe, D. Louer, J. Lucas and A. J. Leonard, *J. Am. Ceram. Soc.*, 1983, **66**, 523.
12 G. Etherington, L. Keller, A. Lee, C. N. J. Wanger and R. M. Almeida, *J. Non-Cryst. Solids*, 1984, **69**, 69.
13 J. H. Simmons, C. J. Simmons, R. Ochoa and A. C. Wright, in ref. 4, p. 37.
14 Y. Kawamoto, T. Horisaka, K. Hirao and N. Soga, *J. Chem. Phys.*, 1985, **83**, 2398.
15 C. C. Phifer, C. A. Angel, J. P. Laval and J. Lucas, *J. Non-Cryst. Solids*, 1987, **94**, 315.
16 F. Ma, Z. Shen, L. Ye, M. Zhang, K. Lu and Y. Zhao, *J. Non-Cryst. Solids*, 1988, **99**, 387.
17 W. C. Wang, Y. Chen and T. D. Hu, *Phys. Status Solidi*, 1993, **136**, 301.
18 W. C. Wang, Y. Chen and T. D. Hu, *J. Phys.: Condens. Matter*, 1994, **6**, 2159.
19 G. E. Walrafen, M. S. Hokmabadi, S. Guha, P. N. Krishnan and D. C. Tran, *J. Chem. Phys.*, 1985, **83**, 4427.
20 S. Aasland, M.-A. Einarsrud, T. Grande and P. F. McMillan, *J. Phys. Chem.*, 1996, **100**, 5457.
21 I. C. Lin, A. Navrotsky, J. Ballato and R. Riman, *J. Non-Cryst. Solids*, 1997, **215**, 113 and refs. therein.
22 T. Grande, S. Aaslund and S. Julsrud, *J. Am. Ceram. Soc.*, 1997, **80**, 1405.
23 L. M. Toth and J. B. Bates, *Spectrochim. Acta*, *Part A*, 1974, **30**, 1095.
24 V. Dracopoulos, Ph.D. Thesis, Department of Chemical Engineering, University of Patras, 2000 (in Greek, containing figures and tables with English labellings).
25 T. Materne and B. Gilbert, *Appl. Spectrosc.*, 1990, **44**, 299.
26 R. E. Thoma, in *Advances in Molten Salt Chemistry*, J. Braunstein, G. Mamantov and G. P. Smith, Plenum Press, New York, 1975, vol, 3, p. 275.
27 G. Brunton, *Acta Crystallogr.*, *Sect. B*, 1973, **29**, 2294.
28 Von R. Hoppe and B. Mehlhorn, *Z. Anorg. Allg. Chem.*, 1976, **425**, 200.
29 W. H. Zachariasen, *Acta Crystallogr.*, 1954, **7**, 792.
30 D. M. Yost, C. C. Steffins and S. T. Gross, *J. Chem. Phys.*, 1934, **2**, 311.
31 V. Dracopoulos, B. Gilbert, B. Borrensen, G. M. Photiadis and G. N. Papatheodorou, *J. Chem. Soc.*, *Faraday Trans.*, 1997, 3081 and refs. therein; V. Dracopoulos, B. Gilbert and G. N. Papatheodorou, *J. Chem. Soc.*, *Faraday Trans.*, 1998, **94**, 2601; G. M. Photiadis, B. Borrensen and G. N. Papatheodorou, *J. Chem. Soc.*, *Faraday Trans.*, 1998, **94**, 2605.
32 Ya. A. Buslaev, V. I. Pachomov, V. P. Tarasov and V. N. Zege, *Phys. Status Solidi*, 1971, **44**, K13; E. C. Reynhardt, J. C. Pratt, A. Watton and H. E. Petch, *J. Phys. C: Solid State Phys.*, 1981, **14**, 4701.
33 G. W. Drake, D. A. Dixon, J. A. Sheehy, J. A. Boatz and K. O. Christie, *J. Am. Chem. Soc.*, 1998, **120**, 8392.
34 K. O. Christie, E. C. Curtis and D. A. Dixon, *J. Am. Chem. Soc.*, 1993, **115**, 1520.
35 T. Grande, H. A. Oye and S. Julrsud, *J. Non-Cryst. Solids*, 1993, **161**, 152.
36 P. R. Papiernik, D. Mercurio and B. Frit, *Acta Crystallogr.*, *Sect. B*, 1982, **38**, 2347.
37 K. Mucker, G. S. Smith, Q. Johnson and R. E. Elson, *Acta Crystallogr.*, *Sect. B*, 1969, **25**, 2362.
38 R. A. McDonald, G. S. Sinke and D. R. Stull, *J. Chem. Eng. Data*, 1962, **7**, 83.
39 M. H. Rand, *At. Energy Rev.*, 1974, No. 5.
40 (*a*) A. P. Lane and D. W. A. Sharp, *J. Chem. Soc. A*, 1969, 2942; (*b*) I. W. Forrest and A. P. Lane, *Inorg. Chem.*, 1976, **15**, 265.